

A STUDY OF THE SYNTHESIS OF HECTORITE

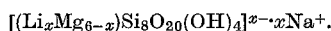
by

W. T. GRANQUIST AND S. S. POLLACK

Mellon Institute, Pittsburgh 13, Pennsylvania

ABSTRACT

Hectorite, a trioctahedral magnesium montmorillonite, has been synthesized at atmospheric pressure and reflux temperature. The reaction mixture was the system $\text{SiO}_2/\text{MgO}/\text{Li}_2\text{O}$ (or $\text{LiF}/\text{Na}_2\text{O}$) in a large excess of water. The starting ratios were based on the following formula for the mineral



Li^+ has been found to accelerate the crystallization, and reasons for this effect are considered. Lowering of the pH of the reaction mixture by the use of alkali metal fluorides rather than hydroxides, resulting in an increase in the solubility of $\text{Mg}(\text{OH})_2$, also caused the crystallization of hectorite to proceed more rapidly. The products containing Li^+ and F^- proxying for Mg^{2+} and OH^- , respectively, were found to be most like natural hectorite.

The time-dependent data obtained in this work were rationalized on the basis of a postulated appearance of hectorite embryos in the dilute aqueous solution of Mg^{2+} , OH^- and SiO_2 , followed by growth of this material to crystalline hectorite by transfer of components from solution to the solid phase.

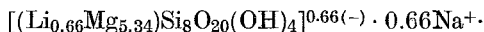
Strese and Hofmann (1941) also conducted synthesis work in this area. A comparison of the products resulting from the two techniques showed the main difference to be the presence of 00 l spacings in the current product. These earlier workers made a point of the lack of 00 l reflections.

INTRODUCTION

The Research Project at Mellon Institute sponsored by Baroid Division National Lead Co. has been directed of late toward the variation of the physical properties of clay minerals as a function of the nature and extent of isomorphous substitution. As a consequence, considerable effort has been expended in the development of techniques for the synthesis of the clay minerals, with emphasis on hectorite.

The clay mineral occurring at Hector, California, was studied by Foshag and Woodford (1936) and by Nagelschmidt (1938). Noll (1936) studied the synthesis (using high-pressure techniques) of magnesium-containing montmorillonite and extended his work to the magnesium end member of the series. Strese and Hofmann (1941) also conducted extensive synthetic work in this area and included a study of the products obtained from an atmospheric pressure approach. A careful x-ray study of the Hector, California, clay is included in their paper. Their approach will be described in a later section of this paper. Incidentally, Strese and Hofmann discussed the presence of Li^+ in the structure and attribute it to accessory mineral.

In their classification of the montmorillonite minerals, Ross and Hendricks (1945) listed hectorite as a trioctahedral montmorillonite having the formula

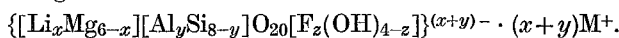


MacEwan (1951) in his discussion of the montmorillonite minerals includes hectorite, and establishes the criterion that the 06 spacing for the trioctahedral montmorillonite should be slightly greater than 1.5 Å, and slightly less than this value for the dioctahedral series. Finally, Eitel (1952) describes compounds prepared by solid state reactions, which he terms "hectorites", and gives the following formula



where the LiF is contained between the layers of the silicate mineral.

In this paper, hectorite is considered to be a trioctahedral montmorillonite mineral of the general formula



The diagnostic criteria are: (a) montmorillonite-like diffraction pattern; (b) 06 spacing > 1.5 Å; (c) no stable anhydride, particularly where F⁻ is not present, resulting in a differential thermal pattern characterized by an extremely sharp exothermic rearrangement to enstatite; (d) rheological properties similar to those of the natural mineral; and (e) analytical and cation exchange results in reasonable accord with the general formula.

The current work has involved the isomorphous replacements shown above and synthesis conditions ranging from reflux temperature and atmospheric pressure to 300°C and *ca.* 1200 psig. The emphasis of this paper is upon the atmospheric pressure synthesis and the effect of varying experimental conditions upon the course of the hectorite crystallization. Some analytical data are presented, but these are few and do not permit evaluation of the subscripts in the above formula. Substitution of Si⁴⁺ by Al³⁺ is not included. These aspects will be considered in future reports.

The authors acknowledge the invaluable aid and encouragement of Dr. J. L. McAtee, Jr., of Baylor University, Dr. E. C. Jonas of the University of Texas, and Drs. J. A. Ferguson and Neill Weber of Mellon Institute and wish to thank Miss Betty Ely and Mr. R. C. Boteler for assistance in the experimental work. The permission of Baroid Division National Lead Co. for publication of these results is gratefully acknowledged.

EXPERIMENTAL PROCEDURES

1. *Synthesis*

The experimental technique involved hydrothermal treatment of an aqueous slurry containing about 10 percent solids. The solids content consisted of freshly precipitated Mg(OH)₂ and silica gel to which was added varying amounts of NaOH and/or LiOH or LiF. The silica gel was prepared by hydrolysis of SiCl₄ (large excess of water) followed by addition of NH₃ (aq) until the solution was strongly alkaline. The gel was filtered and washed

several times to remove Cl^- and NH_4^+ , and the final filter cake was stored under water.

The $\text{Mg}(\text{OH})_2$ was precipitated from a solution of $\text{MgCl}_2 \cdot 6\text{H}_2\text{O}$ by addition of $\text{NH}_3(\text{aq})$; this precipitate also was washed several times to remove most of the Cl^- and NH_4^+ . The two cakes were combined and dispersed in water by means of a Waring Blender. The desired amount of alkali metal hydroxide or fluoride was dissolved in a minimum amount of water and added to the slurry. The mixture was then ready for hydrothermal treatment.

Treatment at atmospheric pressure simply involved refluxing, with stirring, for the required length of time. For convenience, magnetic stirring was employed. At the end of the desired treatment time, the total reaction mixture was filtered through a Buchner funnel, repulped and washed several times, and then dried at 105°C and stored.

2. x-Ray Diffraction Procedures

Crystalline phases in the samples were identified from Debye-Scherrer patterns made with a North American Philips camera having a 114.6 mm diameter. Copper radiation, used with a nickel filter, was employed in all the x-ray work. Integrated intensities of the 13;20 peak of hectorite and the 101 peak of magnesium hydroxide were used as measures of the relative amounts of these components in the various synthetic products. Diffractometer traces were made and the integrated intensity of each peak was calculated by multiplying the width at half the peak height by the intensity above background. Dead-time corrections were made for both peak and background intensities.

In earlier work the 06 hectorite peak was used but not here because of the large overlap of the hectorite peak with the 110 and 111 peaks of magnesium hydroxide in the samples containing large amounts of the latter. The two peaks used in this work were satisfactory even though the fairly sharp magnesium hydroxide peak at $38^\circ 2\theta$ was superimposed on the high-angle tail of the broad hectorite peak located at about 35° . This superposition caused some difficulty in choosing a background line for the hydroxide peak and resulted in some error in the hectorite peak width. Nevertheless, the intensity measurements were reproducible to within 5 percent except for very low intensities where the reproducibility fell to about 10 percent.

A North American Philips diffractometer equipped with a Geiger-counter was used for measuring the diffracted intensities. The copper tube was operated at 35 KV and 20 mA; 1° divergence and scatter slits and a 0.006 in. receiving slit were used with a sample 10.5 mm square and 1 mm thick. All measurements were made with a scale factor of 8 or 4, the multiplier set at 1, a time constant of 2 sec, and a scanning speed of 1° per min.

3. Cation Exchange Capacity and Individual Exchangeable Cations

The cation exchange capacity (CEC) was determined by using a suitable variation of the ammonium acetate technique (Lepper, 1945). The leachates

were examined for Na^+ , Li^+ , and Mg^{2+} by flame photometry and by titration techniques.

4. *Differential Thermal Analysis*

The differential thermal analyses were performed in a multiple sample D.T.A. apparatus using a heating rate of 10°C per min. The range investigated was from ambient temperature to 1000°C .

5. *Wet Analysis*

Standard analytical techniques were used to run total analyses on several of the synthetic products.

6. *Flow Properties of Dispersions*

The product of a 7-day large-scale synthesis (6-liter batch), having an experimental environment similar to that given for the 1B-34 series was spray-dried to a moisture content of 13.6 percent (equilibrium drying at 105°C). Four-percent and 6-percent dispersions (dry basis) in water were prepared using a Waring Blendor. For comparison, a 4-percent dispersion (dry basis) of Hectorite CW, a beneficiated Hector clay, furnished by Baroid Division, was also prepared. Rate of shear-shearing stress curves were determined using a Fann VG meter.

RESULTS

For convenience, most of the experimental data are collected in Tables 1-5 and Figs. 1-3. Discussion of these results is deferred until the next section of the paper. A few additional data will appear in the discussion where pertinent.

DISCUSSION

The Nature of the Synthetic Product

We first examine how well the synthetic materials meet the diagnostic criteria listed in the Introduction. It must be emphasized that all of these criteria were not applied to all the products. For example, while all samples were studied by x-ray and differential thermal techniques, cation exchange results were obtained only for the 1B-34 series, total analyses were performed on only two samples, and flow properties were evaluated for only one sample. Figure 1 contains a comparison of diffractometer traces for the best product (1B-72-7), a typical product (1B-34-7) and Hectorite CW. On this basis it is fair to conclude that the product is montmorillonite-like. Further, in all cases studied the 06 spacing was $>1.5 \text{ \AA}$, justifying the conclusion that the products are trioctahedral.

All the synthetic products gave hk reflections, but well-defined basals were noted only in the 1B-72 series, although the other samples do show broad

TABLE 1.—ENVIRONMENTAL CONDITIONS FOR ATMOSPHERIC PRESSURE SYNTHESSES

Series No.	Feed Composition, Mol Ratio	Solution Composition, g-moles (ions)/l.						
		SiO ₂ /MgO/Li ₂ O/Na ₂ O	OH ⁻	F ⁻	Na ⁺	Li ⁺	Mg ²⁺ (est) ¹	SiO ₂ (est) ²
1B-34	1.5/1.0/0.062/0.062	0.041	0	0.02	0.02	0.71 × 10 ⁻⁸	6.5 × 10 ⁻³	
1B-60	1.33/1.0/0/0.333	0.116	0	0.116	0	0.09 × 10 ⁻⁸	7.0 × 10 ⁻³	
1B-69	1.33/1.0/0/0.124	0.05	0	0.05	0	0.48 × 10 ⁻⁸	6.5 × 10 ⁻³	
1B-71	1.33/1.0/0.124/0	0.05	0	0	0.05	0.48 × 10 ⁻⁸	6.5 × 10 ⁻³	
1B-72	1.33/1.0/0.248(LiF/0	7.28 × 10 ⁻⁴	0.05	0	0.05	3.64 × 10 ⁻⁴	5.8 × 10 ⁻³	
1B-73	1.5/1.0/0.124(LiF)/0.140 ³	0.056	0.025	0.056	0.025	0.382 × 10 ⁻⁸	6.5 × 10 ⁻³	

¹ Estimated from solubility product. ² Correns (1940). ³ Or, SiO₂/(MgO + LiF)/Na₂O = 1.33/1.0/0.124.

maxima at about 10 Å (001) and in the region of 3.2 Å (003). An occasional higher order 00*l* reflection is also seen; for example, from the Debye-Scherrer photograph 002, 003, and 005 reflections were observed in the case of sample

TABLE 2.—DISAPPEARANCE OF Mg(OH)₂ AS A FUNCTION OF TIME AT REFLUX

Series No.	Days at Reflux	D.T.A.		x-Ray	
		Area, Mg(OH) ₂ Endotherm, cm ²	Rel. Am't Mg(OH) ₂	Mg(OH) ₂ (101) Integrated Area, Arbitrary Units	Rel. Am't. Mg(OH) ₂
1B-34	0	1.35	1.0	2432	1.0
	1	0.862	0.639	1118	0.46
	2	0.454	0.348	550	0.23
	3	0.165	0.126	—	—
	5	0.033	0.024	—	—
	7	—	—	—	—
1B-60	0	1.93	1.0	2797	1.0
	1	1.70	0.882	2592	0.93
	3	1.22	0.632	1718	0.61
	5	0.553	0.286	1136	0.41
	7	0.625	0.324	1292	0.46
	—	—	—	—	—
1B-69	0	1.33	1.0	2432	1.0
	1	0.897	0.664	1936	0.80
	3	0.342	0.253	580	0.24
	5	0.236	0.175	—	—
	7	0.142	0.105	—	—
	—	—	—	—	—
1B-71	1	0.746	0.552	1600	0.66
	3	0.036	0.027	—	—
	5	0.013	0.01	—	—
	7	—	—	—	—
1B-72	1	No detectable amount in any treated samples	—	No detectable amount in any treated samples	—
	3				
	5				
	7				
1B-73	1	0.286	0.211	544	0.22
	3	—	—	—	—
	5	—	—	—	—
	7	—	—	—	—

1B-34-7. As will be discussed later, glycerol solvation of sample 1B-72-7 gave a well-defined 00*l* series to the 6th order.

Figure 2 presents differential thermal curves for a typical feed gel, for Hectorite CW, and for two synthetic products, one of which contains some

replacement of OH^- by F^- . This fluoride-containing product is very similar to the natural hectorite, as might be expected because natural hectorite is known to contain F^- proxying for OH^- . It is of interest that neither of

TABLE 3.—CRYSTALLIZATION OF HECTORITE AS A FUNCTION OF TIME AT REFLUX

Series No.	Days at Reflux	Hectorite 13;20 Peak			Rel. Am't. Hectorite (Referred to 1B-72)
		Intensity cps	Width mm	Integrated Intensity	
1B-34	1	19	60	1140	0.21
	2	47	49.5	2327	0.43
	3	62	51	3162	0.59
	5	60	45.5	2730	0.51
	7	66	46.5	3069	0.57
1B-60	1	28	58	1624	0.30
	3	39	55	2145	0.40
	5	52	58	3016	0.56
	7	47	59	2773	0.51
1B-69	1	25	56.5	1413	0.26
	3	66	53.5	3531	0.65
	5	68	57.5	3910	0.72
	7	74	56.0	4144	0.77
1B-71	1	24	62.0	1488	0.28
	3	67	58.0	3886	0.72
	5	77	56.0	4312	0.80
	7	80	58.0	4640	0.86
1B-72	1	90	55.5	4995	0.93
	3	96	57.0	5472*	1.0
	5	99	55.0	5445*	—
	7	96	55.0	5280*	—
1B-73	1	53	51.0	2703	0.50
	3	71	51.0	3621	0.67
	5	85	53.0	4505	0.83
	7	83	54.0	4482	0.83
Hectorite CW (Beneficiated Hector Clay)		75	38.5	2888	—

* 5399 av.

these two fluoride-containing samples demonstrates the anhydride instability and strongly exothermic rearrangement to enstatite that is characteristic of the products containing no such replacement. Presumably, this is because

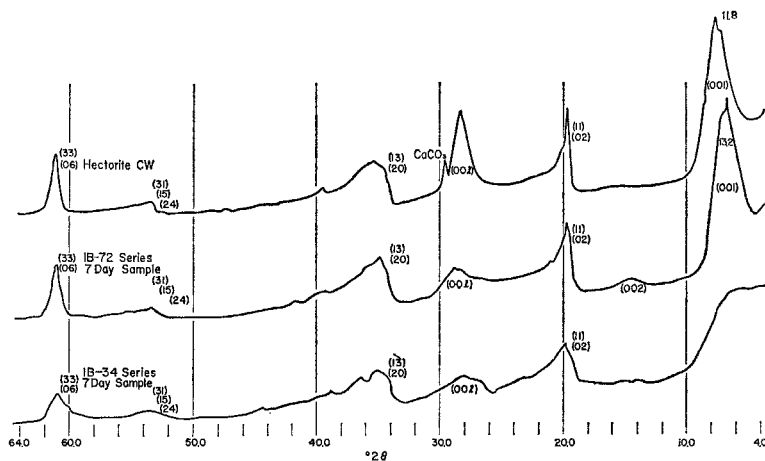


FIGURE 1.—Typical diffractometer traces, synthetic and natural hectorite.

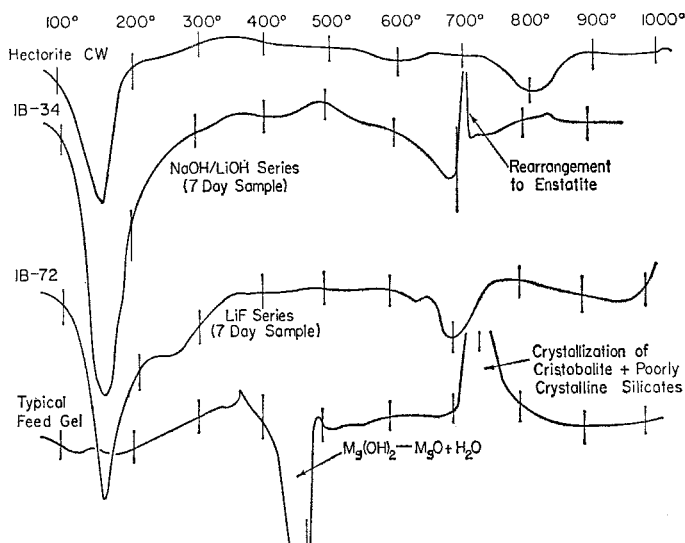


FIGURE 2.—Typical differential thermal patterns.

the fluoride not only decreases the number of hydroxyls present, but also inhibits the interaction of neighboring hydroxyls to produce water and the anhydride. In the non-fluoride products, the high temperature phases were, in general, enstatite as a major phase and α -cristobalite as a minor phase; if F^- is present, the major phase becomes meso-enstatite (ASTM Card 3-0523) with the minor phases α -cristobalite plus an 8.4 Å mineral probably similar

to fluo-tremolite. The fluoride-containing hectorites will be discussed in detail in a future paper.

Finally, consideration of Tables 4 and 5 shows that the synthetic products are chemically similar to natural hectorite (incidentally, the natural hectorite analysis chosen does not demonstrate the presence of F^-) and have

TABLE 4.—TYPICAL ANALYTICAL DATA FOR SYNTHETIC HECTORITES

Percent	Equiv. to 1B-34-7d ¹	Equiv. to 1B-72-7d ¹	Hectorite ²
SiO ₂	57.8	64.5	59.4
MgO	27.41	25.05	28.5
Fe ₂ O ₃	0.41	0.26	0.33
R ₂ O ₃	—	—	0.15
Li ₂ O	1.72	1.96	1.35
Na ₂ O	1.71	1.78	3.04
Comb. H ₂ O	9.18	7.28	6.19
Li ⁺ (exch.)	N.F.	0.12	—
Na ⁺ (exch.)	1.27	1.32	—
F ⁻	—	1.53	—

¹ These particular samples involved identical reaction conditions as series numbers given except that diatomaceous earth was used as a source of silica. The iron shown is a result of this change.

² Recalculated from Kerr, Hamilton and Pill (1950, p. 55).

TABLE 5.—VARIATION OF CATION EXCHANGE PROPERTIES WITH SYNTHESIS TIME; 1B-34 SERIES

Time at Reflux, days	Milliequivalents/100 g Dry Clay			
	C.E.C.	Mg ²⁺	Na ⁺	Li ⁺
1	36.7	337	26.6	21.0
2	38.1	204	24.1	22.5
3	46.1	74.4	42.6	38.2
5	57.2	26.7	79.3	64.3
7	57.9	22.3	71.4	40.8

similar cation exchange properties. In Table 5, the fact that the sum of the exchangeable cations is greater than the exchange capacity simply indicates the presence of soluble material. The decrease in Mg²⁺ with reaction time is another measure of the disappearance of solid Mg(OH)₂. Figure 3 clearly illustrates the rheological similarity of aqueous dispersions of synthetic and natural hectorite. We conclude that the synthetic technique described yields clay-like products that are justifiably termed hectorites.

The high-temperature behavior of the LiOH series (1B-71) deserves special mention. Figure 4 shows the pertinent portions of the thermograms. The 3- and 7-day samples are the same as the 5-day sample illustrated. The 1-day sample is distinctly different from the other three. This 1-day product shows a slight dehydroxylation endotherm followed by an exotherm characteristic of rearrangement to enstatite; in this respect it is similar to the "normal" samples. The difference lies in the second high-temperature exotherm located at 840°C. Contrast this result with the results found for the

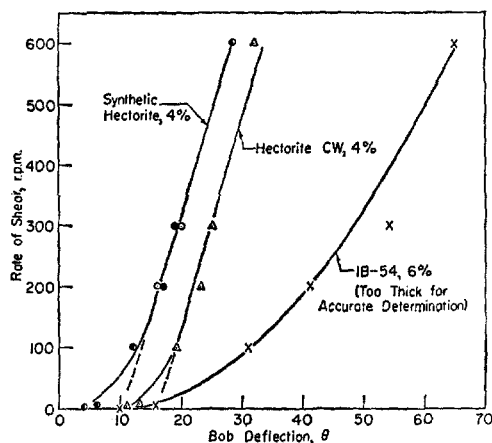


FIGURE 3.—Flow properties of synthetic and natural hectorite.

other three samples. In these cases there exists a reproducible, very sharp endotherm in the dehydroxylation region, followed by the characteristic exotherm for the enstatite formation. This exotherm is followed at 920°C by a second endotherm, and not an exotherm as in the 1-day sample. x-Ray examination indicated that in all the heated samples the major phase was enstatite. In the 1-day sample both quartz and cristobalite are present as minor phases in approximately equal amounts, but in the other samples, quartz is present only as a trace and the minor phase is predominantly cristobalite. These phases do not account for all the lines in the powder photograph, so it is possible that other components may also be present.

Therefore, it is tempting to attribute the second high-temperature endotherm to the transition quartz/cristobalite (5-day sample, Fig. 4), and the second high-temperature exotherm (1-day sample, Fig. 4) to the crystallization of quartz. It is recognized that many objections exist to such an interpretation. Note that this behavior occurs only in the case of greatest concentration of Li^+ , together with no F^- . The high-temperature phases are summarized in Table 6.

Kinetics and Mechanism

The title of this section is presumptuous because the following discussion contains more questions about the mechanism of the process than it does explanations. The gross kinetic data are contained in Tables 2 and 3, and in

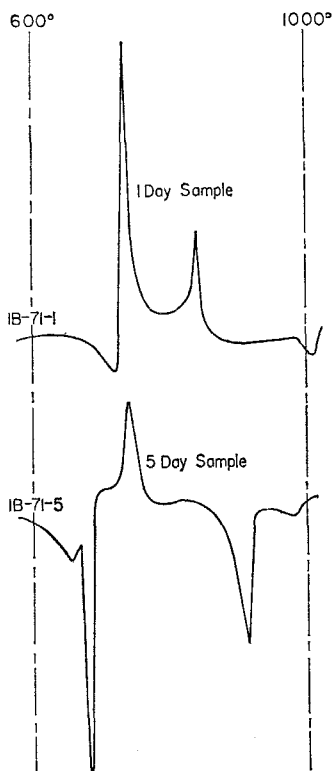


FIGURE 4.—High temperature differential thermal patterns for LiOH series.

Figs. 5–7. Figure 5 illustrates a typical “family” of $\text{Mg}(\text{OH})_2$ endotherms used for determination (supported in part by x-ray data) of the amount of $\text{Mg}(\text{OH})_2$ present at a given stage of the reaction. Figures 6 and 7 present the relative amounts of hectorite and magnesium hydroxide as functions of reaction time. We now try to develop a mechanism that will explain these data; we do not succeed, but the analysis serves a useful purpose in that it illustrates the complexity of the problem and should serve as a stimulus for additional work with this system.

The assumed process can be summarized as follows:

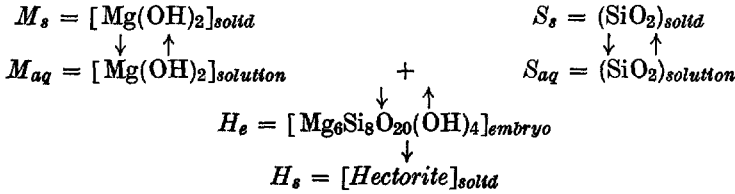


TABLE 6.—HIGH TEMPERATURE PHASES

Series No.	Ions Present Other than Mg ²⁺ , Si ⁴⁺ , O ²⁻		Phases	
	Cations	Anions	Major	Minor
1B-34 (7 day sample)	Li ⁺ , Na ⁺	OH ⁻	enstatite	cristobalite
1B-60* (1 day sample)	Na ⁺	OH ⁻	forsterite	enstatite
1B-60 (7 day sample)	Na ⁺	OH ⁻	forsterite	enstatite
1B-69* (7 day sample)	Na ⁺	OH ⁻	enstatite	cristobalite
1B-71 (1 day sample)	Li ⁺	OH ⁻	enstatite	quartz = cristobalite (possibly another phase)
1B-71 (7 day sample)	Li ⁺	OH ⁻	enstatite	quartz ≪ cristobalite (possibly another phase)
1B-72 (7 day sample)	Li ⁺	F ⁻ , OH ⁻	meso-enstatite	cristobalite + an 8.4 Å mineral probably similar to fluo-tremolite
1B-73 (7 day sample)	Li ⁺ , Na ⁺	F ⁻ , OH ⁻	meso-enstatite	cristobalite + an 8.4 Å mineral probably similar to fluo-tremolite
1B-73-0 (feed sample)	Li ⁺ , Na ⁺	F ⁻ , OH ⁻	enstatite	cristobalite
1B-34-0 (feed sample)	Li ⁺ , Na ⁺	OH ⁻	forsterite = enstatite	cristobalite > quartz

* Starting conc. OH⁻ (in solution) for 1B-60 approximately 3 × that of 1B-69.

We now attempt to simplify this representation. Consider the saturated solution concentrations of Mg²⁺ and SiO₂ contained in Table 1. Calculation of the SiO₂/Mg²⁺ ratio gives results of the order of 10⁶ for all cases except the 1B-72 series where the ratio is of the order of 10. Thus, to the assumption that the hectorite is crystallizing from solution we add the statement that this large excess of silica over Mg²⁺ causes the crystallization to be dependent

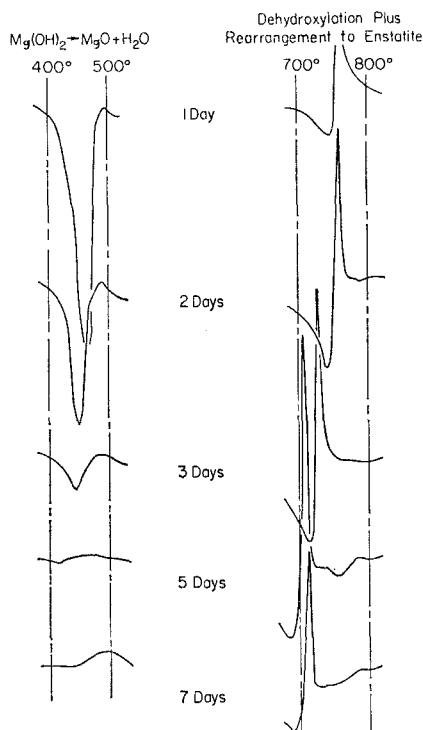


FIGURE 5.—D.T.A. summary, IB-34 series.

only on the concentration of M_{aq} . Therefore, in the following discussion we are concerned only with the role of magnesia. Now, M_{aq} is constant at equilibrium and is controlled by the solubility product of $Mg(OH)_2$, and thus, by the amount of OH^- added. We can apply the steady-state approximation for H_e , with the final result that the rate of disappearance of solid $Mg(OH)_2$ and the rate of appearance of hectorite should be equal, or

$$\frac{d[H_s]}{dt} = -\frac{d[M_s]}{dt}$$

For the solution process,

$$-\frac{d[M_s]}{dt} = (\text{constants}) [M_s], \quad (1)$$

where the term $[M_s]$ refers to the "active mass" of the solid. Integration of (1) leads to the usual first order rate expression:

$$\ln \frac{[M_s]}{[M_s]^0} = -(\text{constants}) t. \quad (2)$$

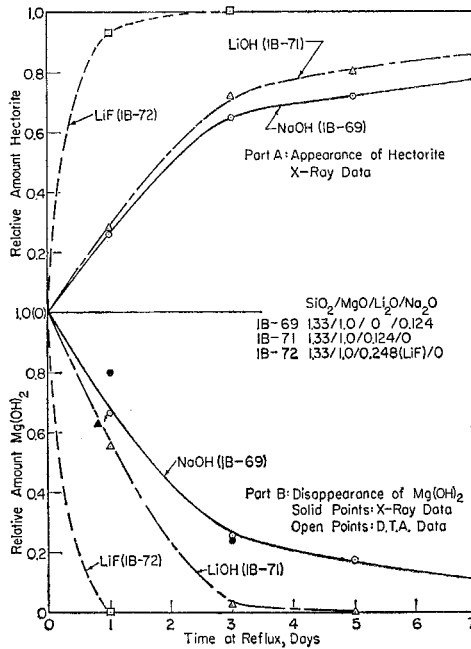


FIGURE 6.—Time dependency of hectorite crystallization.

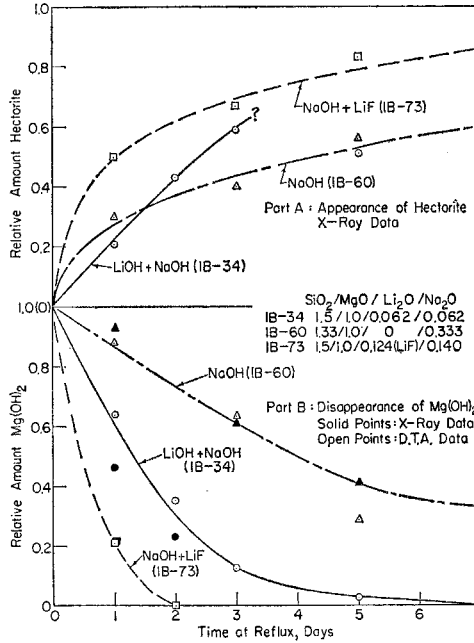


FIGURE 7.—Time dependency of hectorite crystallization.

We must now inquire into the meaning of $[M_s]$, the "active mass," as applied to this specific case. Since this reaction is heterogeneous, the most logical choice for active mass would be the surface of the solid $\text{Mg}(\text{OH})_2$. To complete the discussion of this model, therefore, we need an idea of the weight (or volume) to surface dependence. This can be expressed without recourse to a specific geometrical model by an equation of the type

$$[M_s] = [M_t]^n \quad (3)$$

where $[M_t]$ is the weight concentration of $\text{Mg}(\text{OH})_2$ and n is some number. We suspect that $n = \frac{1}{2}$ because of the CdI_2 -like structure of brucite, with a greater rate of solution along the Mg^{2+} layer than in a direction perpendicular

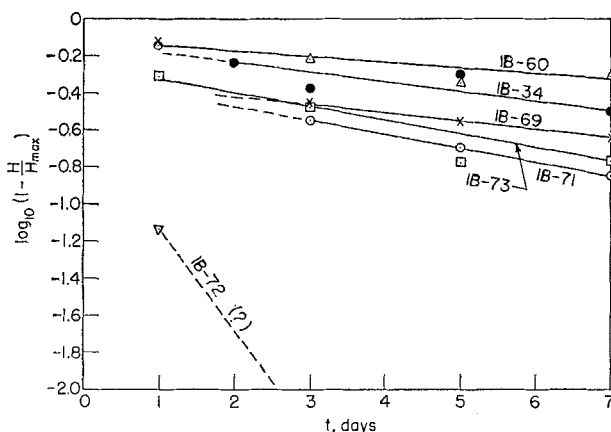


FIGURE 8.—First order rate plots, hectorite formation.

to these layers. If we assume a spherical particle with isotropic rate of solution, then $n = \frac{3}{2}$. Keeping the general form (3), eq. (2) becomes:

$$\ln \frac{[M_t]}{[M_t]^0} = \frac{-(constants)}{n} t = -(G)t. \quad (4)$$

Further, the units of $[M_t]$ and $[H]$ can be so chosen that $[M_t] = [H]_{max} - [H]$, neglecting the term M_{aq} , and we obtain

$$\ln \frac{[H]_{max} - [H]}{[H]_{max}} = -(G)t. \quad (5)$$

Therefore, we can examine the hectorite and $\text{Mg}(\text{OH})_2$ data by first-order rate plots such as (4) and (5) and arrive at some conclusion about the validity of the mechanism (Figs. 8 and 9).

Two disturbing factors arise from these plots: (1) The best straight lines for the hectorite plots do not pass through zero and, (2) the slopes of the

hectorite and magnesia lines for a given series are not equal as demanded by our simple analysis. The values of these slopes and pertinent solution data are contained in Table 7. We first discuss Table 7 and then try to rationalize the two points above.

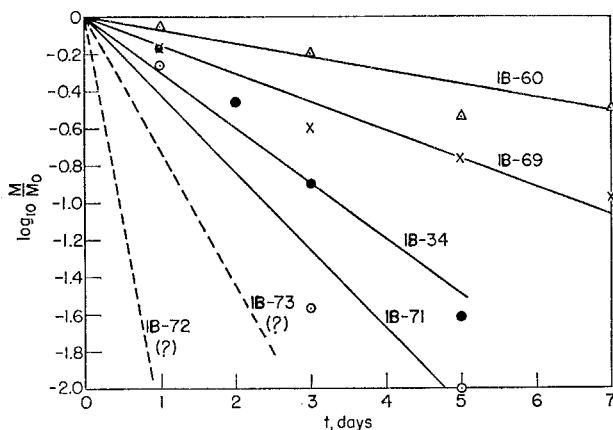


FIGURE 9.—First order rate plots, $\text{Mg}(\text{OH})_2$ dissolution.

TABLE 7.—SUMMARY OF RATE AND ENVIRONMENTAL DATA FOR HECTORITE SYNTHESIS

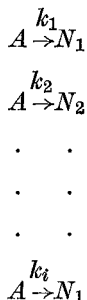
	Series No.	Starting Solution Composition, g-moles/l.				Constant, $\text{Mg}(\text{OH})_2$ Plot	Constant, Hectorite Plot	
		$[\text{OH}^-]$	$[\text{F}^-]$	$[\text{Li}^+]$	$[\text{Na}^+]$			$[\text{Mg}^{2+}]$
Increasing Rate ↓	1B-60	0.116	0	0	0.116	0.09×10^{-8}	0.07	0.033
	1B-69	0.05	0	0	0.05	0.48×10^{-8}	0.15	0.044
	1B-34	0.041	0	0.02	0.02	0.71×10^{-8}	0.30	0.053
	1B-71	0.05	0	0.05	0	0.48×10^{-8}	0.416	0.074
	1B-73	0.06	0.025	0.025	0.06	0.38×10^{-8}	~ 0.7 (?)	0.074
	1B-72	$\sim 10^{-5}$	0.06	0.05	0	3.64×10^{-4}	~ 2 (?)	0.56

Interestingly, both sets of constants arrange the series in the same order and permit certain conclusions about the effect of the environmental conditions upon the rate of hectorite crystallization. For example, consider series 1B-60 and 1B-69. Here the only difference is about a twofold change in initial (OH^-) concentration. The result of the higher (OH^-) concentration for 1B-60 is a decrease in the rate of hectorite formation and can be correlated with the solubility product for $\text{Mg}(\text{OH})_2$ and the common-ion effect. Similarly, in 1B-69 and 1B-71 the only change is the use of LiOH in the latter case instead of NaOH as in the former and the results indicate that the Li^+

increases the rate of crystallization. The other series support these conclusions, particularly 1B-72, in which the use of Li^+ resulted in extremely rapid conversion to hectorite, a combined result of the high Mg^{2+} concentration in solution and the presence of Li^+ . This beneficial effect of Li^+ probably results from an over-all improvement in the energetics of the crystallization due to occasional replacement of Mg^{2+} by Li^+ throughout the structure.

The fact that the two sets of slopes do not even approximately coincide is disturbing in that it implies that solid $\text{Mg}(\text{OH})_2$ is disappearing much faster than hectorite is appearing. This situation would seem to be impossible on the basis of the equilibria postulated earlier in this section. It is important to note that even in a set of competitive first order or pseudo-first order reactions, one of which is the hectorite crystallization, the slopes of the plots of $\ln(M/M_0)$ and $\ln(1-H/H_{max})$ vs. time must be equal. This fact can be established by the following general approach.

We consider a set of i first order, parallel, competitive reactions



and write the expression for A as

$$-\frac{dA}{dt} = k_1A + k_2A + \dots + k_iA = \sum_i k_iA$$

which integrates to $A = A_0 \exp(-\sum_i k_i t)$. Thus, a plot of $\ln A/A_0$ vs. t will have a slope equal to $-\sum_i k_i$. The rate expression for any given product N_i is written as

$$+\frac{dN_i}{dt} = k_iA = k_iA_0 \exp(-\sum_i k_i t)$$

which integrates to $N_i/N_i^\infty = 1 - \exp(-\sum_i k_i t)$, after evaluating the integration constant by setting $t = 0$, and determining N_i^∞ by letting $t \rightarrow \infty$ in the general expression for N_i . Therefore, a plot of $\ln(1 - N_i/N_i^\infty)$ vs. time will also have a slope of $-\sum_i k_i$.

As a result, in order to explain the existing inequality of the slopes, we must postulate the disappearance of $\text{Mg}(\text{OH})_2$ by at least two independent routes, including one reaction leading to hectorite.

One such explanation is to base the hectorite crystallization upon the pseudo-first order reaction in solution between Mg^{2+} and excess silica to form hectorite, and to propose a second reaction involving the deposition of SiO_2 from solution onto the surface of finely divided solid $\text{Mg}(\text{OH})_2$. These reactions can be made independent by assuming that the growth of the hectorite nuclei is rate-controlling and not the $\text{Mg}(\text{OH})_2$ solution process. Thus because of the equilibrium existing between M_{aq} and M_s an increment of hectorite results in a corresponding decrement of M_s , but M_s also disappears independently by a second route, and the net rate of disappearance of $\text{Mg}(\text{OH})_2$ is greater than the rate of hectorite crystallization.

The fact that the hectorite rate plots do not include the origin can be explained by assuming that the rate-controlling growth process initially proceeds much faster (say, at a rate corresponding to the rate of solution of $\text{Mg}(\text{OH})_2$) than it does in the steady state. Such a retardation could be attributed to a dissolution of hectorite, proceeding at a slower rate than the growth process, which would become important only after a certain minimum amount of hectorite had formed.

A most interesting incidental fact that should be mentioned is that periodic x-ray examination of the solid product from several of the runs over a period of some months demonstrated a gradual increase in the amount of hectorite present.

This is illustrated by Plate 1, and best by the 7-day sample of the 1B-60 series. This is the sample that contained the least hectorite and the most $\text{Mg}(\text{OH})_2$ of all the 7-day samples. The 9 months separating the first and last x-ray studies clearly resulted in the appearance of additional crystalline hectorite.

The Work of Strese and Hofmann (1941)

Strese and Hofmann (1941) prepared clay-like magnesium silicates by a process involving the slow addition, with stirring, of a MgCl_2 solution to a boiling potassium silicate solution, and by modifications of this process. This product is described as a "two-dimensional gel" having the *a-b* characteristics of hectorite. Table 8 presents a comparison of the x-ray data for the best products by the two techniques, together with data for natural hectorite.

Both processes involve a slow addition of Mg^{2+} to a large excess of SiO_2 in solution. The present process, involving a transition from solid reactants, through the solution or through a colloidal state, to solid product, is probably more characteristic of the reaction as it occurs in nature. Further, the present technique makes it possible to eliminate any extraneous ions from the reaction and also permits reaction at much lower alkali metal concentration because it is not required that all the silica be in solution. Future plans of

this laboratory include study of the Strese and Hofmann product by current techniques, including determination of the flow properties of a redispersed sample.

TABLE 8.—COMPARISON OF X-RAY DATA FOR NATURAL AND SYNTHETIC HECTORITE

Indices ¹	<i>d</i> (calc) ¹	Natural Hectorite after Hofmann ²	Hofmann's ² Synthetic, 22W2	Present ³ Synthetic, 1B-72-7
11, 02	4.49	4.51 s	4.55 s	4.5 s
13, 20	2.59	2.58 s	2.58 vs	2.6 s
22, 04	2.25	2.25 vw	—	2.25 vw
31, 15, 24	1.703	1.72 mv	1.70 w	1.74 m
33, 06	1.500	1.51 s	1.52 vs	1.53 s
26, 40	1.298	1.31 m	1.31 m	1.31 m
35, 17, 42	1.249	1.26 w	1.29 vvw	1.28 w
08, 44	1.125	1.15 vvw	1.15 vvw	1.18 w
37, 28, 51	1.034	1.05 vvw	—	1.04 w
19, 53, 46	0.982	0.99 mw	0.987 vw	0.98 m
55	0.900	—	—	0.90 w
39, 60	0.8665	0.88 m	0.88 vw	0.875 m

00*l*, *d* variable with percent RH

00 <i>l</i>	<i>d</i>			"Glycerated"
001	9.9	s	none	18.0 100 (I)
002	4.8	w	none	9.20 25
003	3.2	m	none	5.94 10
004	—	—	—	4.55 25
005	1.96	vwv	none	3.57 20
006	—	—	—	3.03 10

¹ MacEwan (1951). MacEwan does not report 00*l*.

² Strese and Hofmann (1941).

³ Taken from Debye-Scherrer patterns.

REFERENCES

- Correns, C. W. (1940) Über die Löslichkeit von Kieselsäure in schwach-säueren und alkalischen Lösungen: *Chem. d. Erde*, v. 13, pp. 92-96.
- Eitel, W. (1952) Synthesis of Fluorosilicates of the Mica and Amphibole Groups: *Proceedings, International Symposium on the Reactivity of Solids*, v. 1, pp. 335-347.
- Foshag, W. F. and Woodford, A. O. (1936) Bentonitic magnesian clay-mineral from California: *Amer. Mineral*, v. 21, pp. 238-244.
- Kerr, P. F., Hamilton, P. K. and Pill, R. J. (1950) Analytical data on reference clay minerals, Sec. 1: Rept. 7, American Petroleum Institute Project 49, pp. 1-69.
- Lepper, H. A., Ed. (1945) *Official and Tentative Methods of Analysis*, Association of Official Agricultural Chemists, Washington, D.C., pp. 13-20.

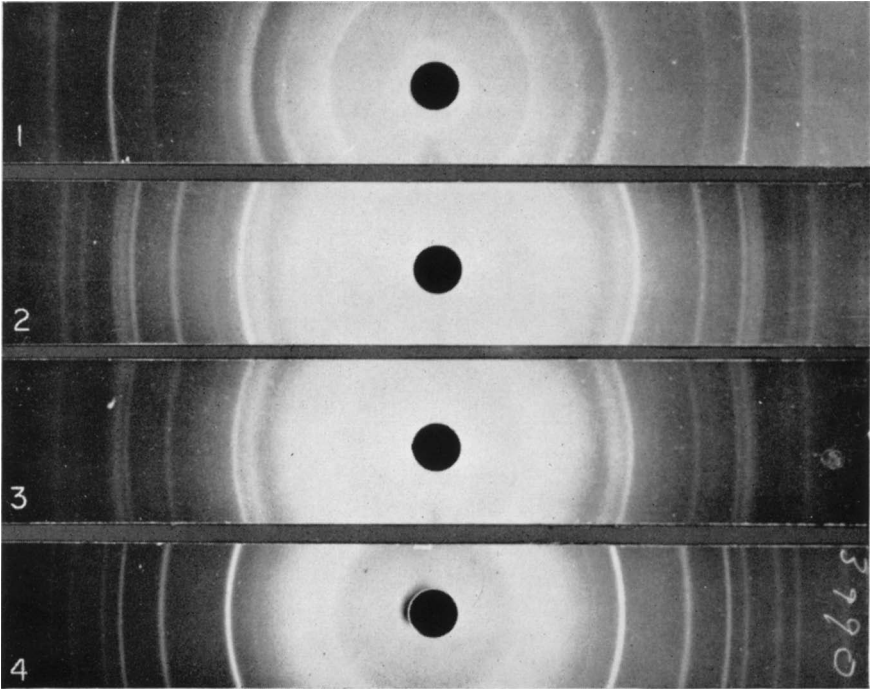


PLATE 1.—Variation in relative hectorite content over a long time period. (1) Hectorite; (2) IB-60-7, March 1959; (3) IB-60-7, August 1959; (4) Magnesium hydroxide.

[facing page 168

- MacEwan, D. M. C. (1951) The montmorillonite minerals (montmorillonoids): in *x-Ray Identification and Crystal Structures of Clay Minerals*, Mineralogical Society, London pp. 86-137.
- Nagelschmidt, G. (1938) On the atomic arrangement and variability of the members of the montmorillonite group: *Mineralog. Mag.*, v. 25, pp. 140-155.
- Noll, W. (1936) Synthese von montmorilloniten: *Chemie der Erde*, v. 10, pp. 129-153
See also Noll, W. (1940) *Angew. Chemie*, v. 53, p. 240.
- Ross, C. S. and Hendricks, S. B. (1945) Minerals of the montmorillonite group, their origin and relation to soils and clays: *U.S. Geol. Survey Prof. Paper* 205-B, pp. 23-79.
- Strese, H. and Hofmann, U. (1941) Synthesis of magnesium silicate gels with two dimensional regular structure: *Z. anorg. Chem.*, v. 247, pp. 65-95.